Functional implications of the localization and activity of acid-sensitive channels in rat peripheral nervous system

Diego Alvarez de la Rosa*, Ping Zhang*, Deren Shao*, Fletcher White†, and Cecilia M. Canessa*‡

Departments of *Cellular and Molecular Physiology, and †Neurology, Yale University School of Medicine, New Haven, CT 06520

Communicated by Joseph F. Hoffman, Yale University School of Medicine, New Haven, CT, December 20, 2001 (received for review October 5, 2001)

Acid-sensitive ion channels (ASIC) are proton-gated ion channels expressed in neurons of the mammalian central and peripheral nervous systems. The functional role of these channels is still uncertain, but they have been proposed to constitute mechanoreceptors and/or nociceptors. We have raised specific antibodies for ASIC1, ASIC2, ASIC3, and ASIC4 to examine the distribution of these proteins in neurons from dorsal root ganglia (DRG) and to determine their subcellular localization. Western blot analysis demonstrates that all four ASIC proteins are expressed in DRG and sciatic nerve. Immunohistochemical experiments and functional measurements of unitary currents from the ASICs with the patch–clamp technique indicate that ASIC1 localizes to the plasma membrane of small-, medium-, and large-diameter cells, whereas ASIC2 and ASIC3 are preferentially in medium to large cells. Neurons coexpressing ASIC2 and ASIC3 form predominantly heteromeric ASIC2–3 channels. Two spliced forms, ASIC2a and ASIC2b, colocalize in the same population of DRG neurons. Within cells, the ASICs are present mainly on the plasma membrane of the soma and cellular processes. Functional studies indicate that the pH sensitivity for inactivation of ASIC1 is much higher than the one for activation; hence, increases in proton concentration will inactivate the channel. These functional properties and localization in DRG have profound implications for the putative functional roles of ASICs in the nervous system.

Acid-sensitive ion channels (ASICs) are channels activated by external protons that belong to the larger family known as degenerins/epithelial Na^+ channel (1). In mammalian organisms, six different proteins arise from four genes. ASIC1α (BNaC2) (2, 3) and ASIC1β (4) are spliced forms of the ASIC1 gene; they differ in the first 172 amino acids. ASIC2a (BNaC1 or MDEG1) (2, 5) and ASIC2b (MDEG2) are spliced forms of the ASIC2 gene; they differ in the first 236 amino acids (6). ASIC2b does not induce current but, with ASIC3, forms functional heteromultimeric channels (6). ASIC3 (DRASIC) (7–9) is activated by protons but not ASIC4 (SPASIC) (10, 11).

Expression of the ASIC genes in sensory neurons and activation by extracellular protons have suggested that they may participate in nociception (12). On the other hand, the structural similarity shared with the degenerins, which are involved in light-touch sensitivity in *Caenorhabditis elegans*, has prompted postulation of a role for the ASICs in mechanoperception (13). The mammalian ASIC2 gene was recently disrupted in mouse (14). Knockout mice did not exhibit a distinct phenotype, but careful examination of the fibers innervating the skin revealed that the low-threshold, rapidly adapting, and, to a lesser degree, slowly adapting mechanoreceptors showed reduced discharge frequency on stimulation when compared with wild-type animals.

Previous publications have reported the distribution of ASICs mRNAs by Northern blot analysis or *in situ* hybridization. By *in situ* hybridization, small neurons exhibit the highest level of ASIC1α mRNA expression in dorsal root ganglia (DRG) (3), whereas ASIC1β is present in 20–25% of both small- and large-diameter neurons (4). Expression of ASIC2b overlaps with ASIC2a in brain but not in DRG that express only ASIC2b (6). ASIC3 mRNA was detected in small-diameter neurons (4, 7). By reverse transcription–PCR, ASIC3 has also been found in non-neuronal tissues such as testis (8) and lung (9). Akopian found a low level of ASIC4 mRNA in DRG (10), whereas Gründer did not detect it (11). Collectively, previous reports are not always in agreement, and conclusions regarding tissue distribution of the ASICs are difficult to make with the current information.

In this work, we have examined the distributions of all the ASIC proteins in DRG by using specific antibodies. In addition, we have studied the activity of the ASIC channels in various populations of freshly isolated DRG neurons by using the patch–clamp technique in the outside-out configuration. Data from these experiments, together with further characterization of functional properties of the ASICs, provide insight on the functional role of these channels in the nervous system.

Materials and Methods

cDNA Constructs. Rat cDNAs from ASIC1, ASIC2, and ASIC4 were cloned by reverse transcription–PCR from adult brain poly(A)$^+$ mRNA by using specific primers with sequences obtained from the data bank. Full-length cDNA from human ASIC3 was purchased from the IMAGE Consortium (Livermore, CA). A FLAG epitope was added to the C termini of each of the four ASIC cDNAs and subcloned into pCDNA3.1. All constructs were sequenced at the Keck Facility at Yale University.

Generation and Affinity Purification of Anti-ASIC Antibodies. Antibodies were generated by s.c. injection of rabbits with glutathione *S*-transferase fusion proteins of the following sequences: R465-C526 (rASIC1), E470-C512 (rASIC2), N474-Q530 (hASIC3), and D471-C539 (rASIC4). Sera were affinity purified by using the corresponding glutathione *S*-transferase fusion peptides bound to Hi-Trap *N*-hydroxysuccinimide-activated agarose columns (Amersham Pharmacia).

Cell Culture and Transfection of Cells. HEK293 cells were cultured on DMEM with 10% FBS. For immunocytochemistry, cells were seeded on glass coverslips coated with poly(D-lysine). Cells were transiently transfected with the cDNAs of ASIC-1, -2, -3, or -4 with Lipofectamine (Life Technologies, Gaithersburg, MD). Freshly isolated DRG cells were prepared as described (15) and maintained up to 36 h at 37°C in a humidified 95% air/5% CO_2 incubator.

Western Blots. HEK293 cells, DRG, or sciatic nerve were homogenized in: 50 mM Tris·HCl, pH 7.5/5 mM EDTA/150 mM

Abbreviations: ASIC, acid-sensitive ion channel; DRG, dorsal root ganglia.

‡To whom reprint requests should be addressed. E-mail: cecilia.canessa@yale.edu.

The publication costs of this article were defrayed in part by page charge payment. This article must therefore be hereby marked "*advertisement*" in accordance with 18 U.S.C. §1734 solely to indicate this fact.

NaCl/1% Triton X-100/Complete protease inhibitors (Roche Molecular Biochemicals). Protein concentration was measured with a BCA assay kit (Pierce). Equal amounts of protein were resolved in SDS-10% polyacrylamide gels and transferred to Immobilon-P membranes (Millipore). After the membranes were blocked with 5% dry milk, they were incubated with a 1:2,000 dilution of the specific purified antibodies at room temperature for 1 to 2 h followed by extensive washes. A 1:10,000 dilution of anti-rabbit horseradish peroxidase-labeled antibody (Sigma) was added and incubated for 1 h. Blots were developed with enhanced chemiluminescence (ECL plus; Amersham Pharmacia).

Immunocytochemistry of Transfected Cells. Transfected HEK293 grown on coverslips were fixed with 4% formaldehyde in PBS, permeabilized with 0.3% Triton X-100 and 0.1% BSA, followed by blocking with 16% filtered goat serum/0.3% Triton X-100/20 mM NaP_i, pH 7.4/150 mM NaCl. Cells were then incubated with 1:200 dilutions of anti-ASIC1, ASIC2-C, or ASIC3 affinity-purified antibodies or 20 μg/ml of FLAG M2 antibody (Sigma) in blocking buffer for 1 h at room temperature. After washes, cells were incubated for 1 h with anti-rabbit fluorescein (Sigma) or anti-mouse rhodamine-conjugated antibodies (Sigma) diluted 1:100. Images were collected with a Zeiss LSM-410 laser-scanning microscope. No signal was observed in nontransfected cells or with omission of the primary antibodies.

Immunohistochemistry of Rat Tissues. Adult male Sprague–Dawley rats were anesthetized with 0.4 ml of Nembutal administered i.p. and perfused transcardially with Ca^{2+}-free Tyrode's solution followed by fixative (4% paraformaldedehyde and 0.2% picric acid in 0.1 M phosphate buffer). DRG were dissected and transferred into 10% sucrose buffer overnight before cutting. Frozen sections (10 or 30 μm) were processed for immunofluorescence histochemistry with single- or double-antibody labeling. Sections were incubated for 16–18 h at 4°C with primary antibody diluted in PBS/0.3% Triton X-100/0.1% BSA/10% goat serum. After rinsing, sections were incubated for 1–2 h with anti-rabbit goat antibody (1:200) Alexafluor (Molecular Probes). Controls were omission of primary antibody or competition with the corresponding fusion protein.

Staining with two rabbit primary antibodies was performed with the Tyramide Signal Amplification Fluorescence System (NEN) according to the protocol provided by the manufacturer. Primary anti-ASIC antibodies and a commercial antibody that recognizes the N terminus of rat ASIC2 (ASIC2-N) (Alomone Laboratories, Jerusalem) were diluted 1:2,000 to 1:6,000. The secondary antibody, biotin-SP-conjugated donkey anti-rabbit IgG (The Jackson Laboratory) was diluted 1:200. Amplification of the first antibody was performed with fluorescein-labeled tyramide. Two blocking steps were added after the first staining was completed: rabbit serum (1:10,000) for 1 h in the blocking solution provided by the TSA Fluorescence System kit followed by anti-rabbit Fab fragments (1:20) (The Jackson Laboratory). After washes, the slides were treated with a different rabbit anti-ASIC antibody. Steps identical to the first staining were used, with the exception that the amplification reaction was performed with cyanine-3-labeled tyramide. The following controls were included in these experiments. Control for the masking steps consisted of omission of the second primary rabbit antibody. To ensure that the horseradish peroxidase used in the first immunostaining had lost its activity, we omitted the horseradish peroxidase in the second immunostaining. To identify populations of sensory neurons, we used antiperipherin (MAB1527, Chemicon) and antineurofilament 200 (MAB1623; Chemicon) diluted 1:200.

Single-Channel Recordings from DRG and Injected *Xenopus* Oocytes. Currents from ASICs were recorded by using the outside-out configuration of the patch–clamp technique as described (16). When indicated, 10 μM ruthenium red was included in the low pH_o solutions. Data were filtered to 5 kHz, digitized at a sampling interval of 200 μs, and stored on a computer hard disk for analysis. For display, data were filtered with a digital Gaussian filter to 0.5 kHz. Composition of the pipette solution (intracellular) was: 120 mM NaGluconate/30 mM NaCl/1 mM $CaCl_2$, pH 7.4. The bath solution (extracellular) was: 150 mM NaCl/1 mM $CaCl_2$ with pH adjusted to 7.4 or 5.0. With these solutions, the reversal potential of Cl^- is -40 mV. Therefore, by holding the membrane potential at -40 mV, the only currents detected are the ones carried by Na^+. All experiments were performed at room temperature.

Two-Electrode Voltage Clamp from *Xenopus* Oocytes. Stage V and VI *Xenopus* oocytes were injected with 2 ng of cRNA from ASIC1, ASIC2, ASIC3 alone, or in various combinations. cRNAs were synthesized from linearized plasmids by using T7 RNA polymerase with the MESSAGEMACHINE kit, according to the provider's instructions (Ambion, Austin, TX). Oocytes were incubated at 19°C for 2–5 days before recordings. Whole-cell currents were measured with the two-microelectrode voltage–clamp technique, as described (16). The composition of the standard bath solution was: 150 mM NaCl/2 mM KCl/1 mM $CaCl_2$, pH adjusted with 10 mM Hepes and 10 mM Mes to the desired value.

Results

Characterization of Anti-ASIC Antibodies. We raised rabbit polyclonal antibodies against the C terminus of ASIC-1, -2, -3, and -4; we chose the C terminus because it is the most divergent region among the ASIC proteins. After affinity purification, the antibodies were examined on Western blots for their ability to recognize the recombinant ASIC proteins and for specificity. Equal amounts of protein from ASIC-transfected HEK293 cells were examined with each of the four ASIC antibodies. The antibodies recognized proteins of the predicted glycosylated molecular weight, as shown in Fig. 1*A*. No crossreactivity was observed with any of the antibodies.

We next examined the antibodies in immunocytochemical experiments. HEK293 cells were transfected with cDNAs of the ASICs tagged with FLAG epitope. Fixed cells were double labeled with the specific ASIC antibodies and a monoclonal FLAG antibody. Fig. 1*B* shows in green the signal provided by ASIC antibodies and in red the ones from the FLAG antibody. Superimposition of the two images by using confocal microscopy indicates colocalization of the two signals (yellow). Control cells did not exhibit immunoreactivity. In transfected cells, most of the signal was in the endoplasmic reticulum, a pattern frequently seen with overexpressed membrane proteins. We will see later that, in native tissues, the ASICs localize to the plasma membrane. The ASIC4 antibody produced a weak signal; therefore, it was not used in further immunohistochemical experiments.

Expression of ASIC Proteins in DRG and Sciatic Nerve. Expression of ASIC proteins in DRG and sciatic nerve was examined by Western blots. Fig. 2 shows that all ASIC genes are expressed in both tissues. The ASIC2 protein was recognized with two different antibodies. The ASIC4 antibody identified two bands, one at the predicted molecular weight and a faint band at a higher molecular weight whose identity is currently undetermined.

Expression of ASIC2 Spliced Isoforms in DRG. Differential splicing of the ASIC2 gene produces the isoforms ASIC2a and 2b, which differ only in their N termini. According to a previous report,

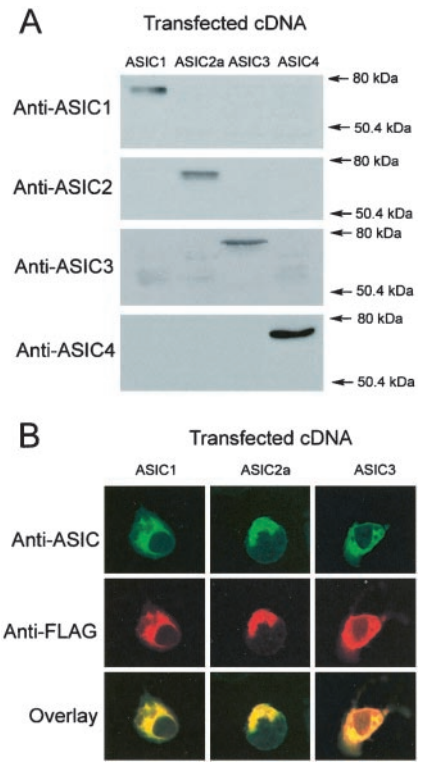

Fig. 1. Characterization of ASIC antibodies. (*A*) Western blots from HEK cells transfected with ASIC-1, -2a, -3, and -4 cDNAs probed with affinity-purified specific antibodies. (*B*) Immunocytochemistry of HEK cells transfected with ASIC-1, -2, and -3 cDNAs tagged with FLAG epitope. (*Top*) Confocal images of cells labeled with the corresponding anti-ASIC antibodies (green); (*Middle*) labeling with monoclonal anti-FLAG antibody (red); (*Bottom*) the merge of the previous two images (yellow).

ASIC2a is expressed in brain but absent in DRG, whereas ASIC2b is expressed only in DRG (7). Because the two ASIC2 antibodies recognize different epitopes, they were used to assess the expression and relative abundance of the two isoforms. The apparent affinities of the antibodies were tested in Western blots containing decreasing amounts of proteins from HEK293 transfected with ASIC2a. Fig. 3*A* shows that the intensity of the anti-ASIC2-N signal is approximately 10-fold stronger than the one produced by anti-ASIC2-C. In contrast, in DRG the anti-ASIC2-C signal is slightly stronger than the one produced by anti-ASIC2-N (Fig. 3*B*). These results indicate that both isoforms are expressed in DRG and that ASIC2b is the most abundant.

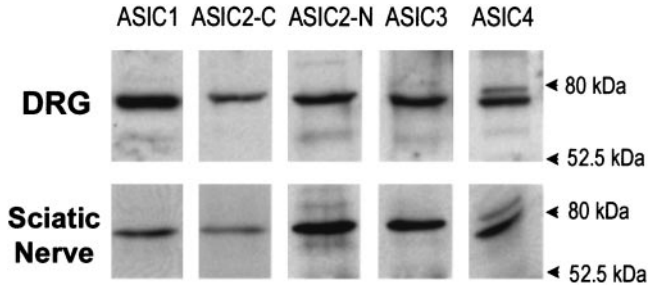

Fig. 2. Western blots of DRG and sciatic nerve. Analysis of 50 and 80 μg of proteins extracted from DRG and sciatic nerve, respectively, with five different antibodies for: ASIC1, ASIC2-C (recognizes the C terminus of ASIC2a and ASIC2b), anti-ASIC2-N (specific for the N terminus of ASIC2a), ASIC3, and ASIC4.

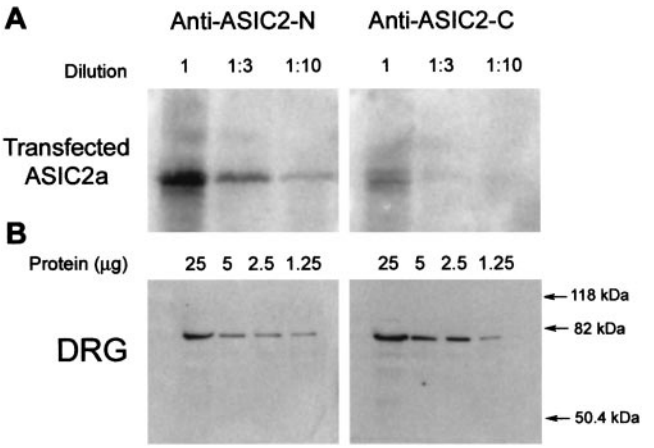

Fig. 3. Apparent affinities of anti-ASIC2-N and anti-ASIC2-C antibodies examined by Western blots. (*A*) Serial dilutions of lysates from HEK transfected with ASIC2a; (*B*) serial dilutions of lysates from DRG. Membranes were probed with ASIC2-N or ASIC2-C antibodies.

Localization of ASIC1, -2, and -3 in DRG by Immunohistochemistry. ASIC antibodies were used alone or with markers specific for small diameter (17) or for medium- to large-diameter cells (18). Fig. 4 shows labeling of DRG with anti-ASIC1 alone (Fig.4*A*) and double labeling with antiperipherin (Fig.4*B*), or with antineurofilament 200 (Fig.4*C*). The ASIC1 antibody (green) labels cells positive for either of the two markers (red). Immunoreactivity was present also in the plasma membrane of peripheral axons (Fig.4*D*).

An antibody against the N terminus has been used to show expression of ASIC2a in the cytoplasm of medium to large DRG neurons (19). Here we investigated two additional questions: first, whether there is a differential distribution of the ASIC2 isoforms in DRG, and second, whether ASIC2 colocalizes with ASIC3.

Staining of DRG with ASIC2-N or ASIC2-C antibodies labeled the plasma membrane mainly of medium-large cells (30–60 μm in diameter) (Fig. 5 *A* and *B*). The result was

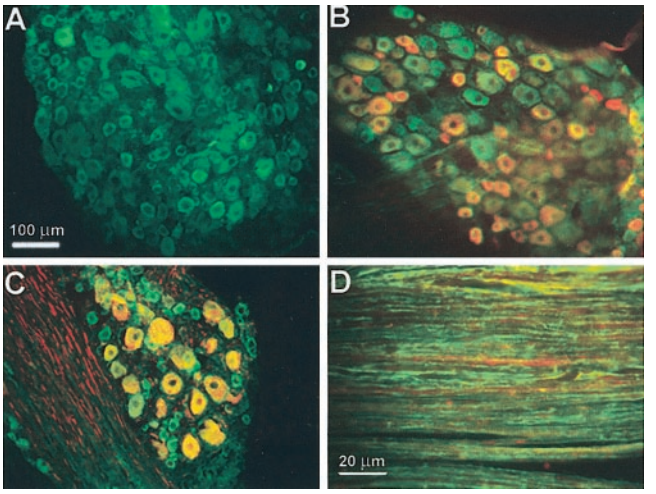

Fig. 4. Immunolocalization of ASIC1 in DRG. (*A*) Staining with ASIC1 antibody. (*B*) Double staining with ASIC1 (green) and monoclonal antiperipherin (red). (*C*) Double staining with ASIC1 (green) and monoclonal antineurofilament 200 (red). (*D*) Section of sciatic nerve labeled with ASIC1 (green) and monoclonal antineurofilament 200 (red). ASIC1 localizes to small-, medium-, and large-diameter cells and overlaps with peripherin or neurofilament 200. In sciatic nerve ASIC1 stains the plasmalemma of axons.

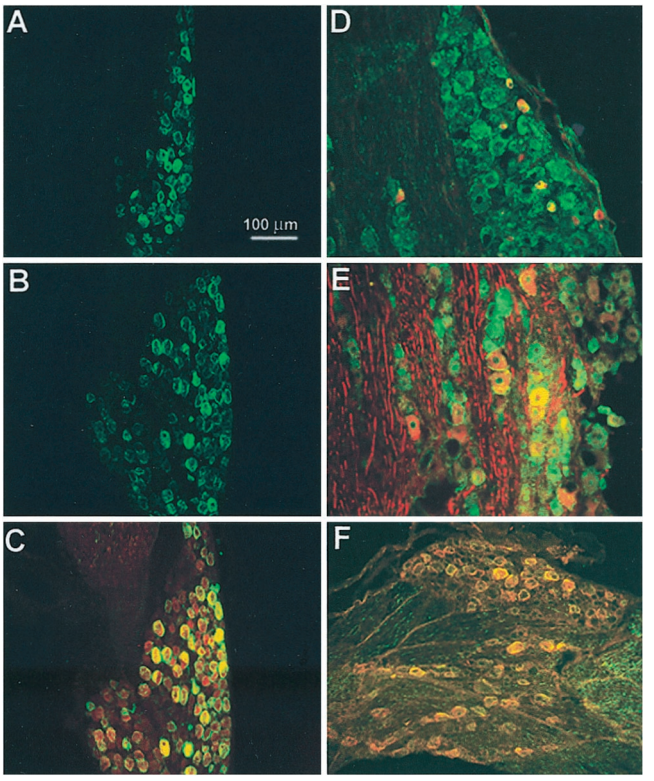

Fig. 5. Immunolocalization of ASIC2 and ASIC3 in DRG. (*A*) Staining of DRG with ASIC2-N antibody; (*B*) staining with ASIC2-C; (*C*) double staining with ASIC2-N (red) and ASIC2-C (green); (*D*) double staining with ASIC3 (green) and anti-peripherin monoclonal antibody (red) or with (*E*) antineurofilament 200 monoclonal antibody (red). (*F*) Double staining with ASIC2-C (green) and ASIC3 (red) antibodies.

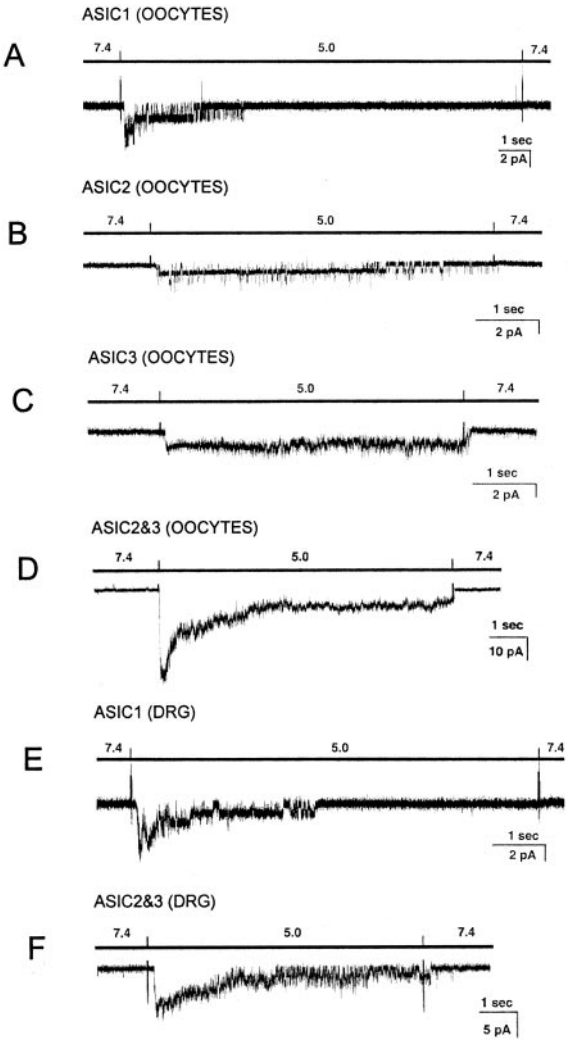

Fig. 6. Representative examples of acid-activated currents in oocytes injected with different ASIC cRNAs and in freshly isolated neurons from DRG. Recordings were obtained from outside-out patches held at −40 mV. Bars above traces indicate the change in pH_0. The spikes in the records are artifacts introduced by the change of solution. Bars indicate the scale for time and current amplitudes. Currents from ASIC1 (*A*), ASIC2 (*B*), ASIC3 (*C*), and ASIC2–3 (*D*) expressed in oocytes. (*E*) Currents with characteristics of ASIC1 in small cells from DRG. (*F*) Currents with characteristics of ASIC2–3 in medium-large DRG cells.

reproduced with the two ASIC2 antibodies. We then examined the distribution of the ASIC2 isoforms in double-staining experiments by using the tyramide amplification system with anti-ASIC2N (red) and anti-ASIC2C (green). In most cells the signals colocalized (Fig. 5*C*); few neurons were stained with only one of the antibodies.

ASIC3 was primarily present in medium-large neurons. In many cells it colocalized with neurofilament 200 but also with a few small peripherin-positive cells (Fig. 5 *D* and *E*).

We then examined whether ASIC2 and ASIC3 colocalize in the same population of cells. Double labeling with anti-ASIC2-C (green) and anti-ASIC3 (red) by using the tyramide amplification system showed predominantly yellow fluorescent cells (90% overlap), indicating that the two proteins are in the same population of cells (Fig. 5*F*).

Functional Characterization of Unitary ASIC Currents Expressed in Oocytes. The previous experiments showed that DRG express at least five different ASIC proteins. We asked whether immunoreactivity correlates with the presence of functional channels by using outside-out patches. The advantage of studying unitary currents over whole-cell currents (20, 21) is the ability to identify unambiguously the type of ASIC channel. However, we first had to establish the criteria to distinguish each of the ASIC channels. This was done in oocytes injected with various combinations of ASIC cRNAs.

Oocytes expressing ASIC1α exhibit transient currents that completely inactivate on the continual presence of low pH_o. Extensive characterization of unitary currents from recombinant rASIC1 will be published elsewhere (P.Z. and C.M.C., unpublished work). A representative example of ASIC1α expressed in oocytes is shown Fig. 6*A*.

Oocytes injected with ASIC2a expressed channels that partially inactivate at low pH_o. Fig. 6*B* shows a patch containing two ASIC2 channels with initial high NP_o that decreases during pH_o 5.0 pulse giving the sustained component of the current. Injection of ASIC3 cRNA produced noninactivating channels as shown in Fig. 6*C*. Oocytes coinjected with ASIC2a and ASIC3 expressed channels with properties and kinetics that have been extensively examined (16) (Fig. 6*D*).

Oocytes coinjected with ASIC1 and ASIC3 expressed two populations of channels distinctive of ASIC1 and ASIC3, indicating that they do not coassemble when expressed in the same cells.

The main differences among the ASIC channels were the inactivation properties and channel kinetics. These features were used as criteria to distinguish the ASICs in native tissues.

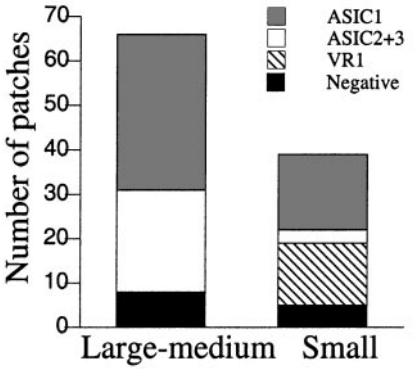

Fig. 7. Frequency of ASIC channels in DRG neurons. Stack columns represent the frequency of finding various types of ASICs in outside-out patches from freshly isolated DRG cells. Cells were classified as small or medium-large by visual inspection under the microscope of the patch-clamp setup. Channels were assigned to categories according to the properties of inactivation, single channel kinetics, current sublevels, and block by ruthenium red. The conditions of the experiments were the same as in oocytes.

Functional Identification of ASIC Channels in Freshly Isolated DRG Neurons. DRG neurons attached to coverslips were classified according to their size into small (<30 μm in diameter) or medium-large (30–50 μm) by inspection under the microscope of the patch–clamp setup equipped with a calibrated ruler. Outside-out patches were obtained from the soma. Channels were activated by rapid perfusion with pH_o 5.0 solutions. Because some neurons express VR1 (22), we added the blocker ruthenium red to the low pH_o solutions (23). This compound does not affect any of the ASICs.

The frequency of finding acid-activated channels in the patch was high (0.87) and, in most cases, multiple channels were detected in the patch, indicating that ASICs are abundant in the plasma membrane of the soma. ASIC1 was the most frequently detected channel (Fig. 6*E*). Channels with properties characteristic of heteromeric ASIC2–3 were the second most frequently recorded (Fig. 6*F*). The frequency of finding ASIC channels in cells classified according to diameter is indicated in Fig. 7. In medium-large cells, we found ASIC1 channels in 35 of 66 cells and ASIC2–3 in 23 of 66 cells. Often, only one type of channel was seen in the patch, but occasionally we saw both ASIC1 and ASIC2–3 in the same patch. In small-diameter cells, the most frequent channel was ASIC1 (17 of 39). ASIC2–3 channels were found less frequently (3 of 39). Only small cells expressed VR1 (14 of 39), which was distinguished from all of the ASICs by kinetics and inhibition by ruthenium red.

Proton Dependence of Activation and Inactivation of ASIC1. We have consistently observed a lower proton sensitivity of rASIC1 in native tissues and in heterologous expression systems than was reported originally (pH_{50} = 6.2) (3). To measure the apparent K_d for protons, peak whole-cell inward currents were induced by rapid changes of the bathing solution from 7.4 to solutions of lower pH_o. The data were fitted to the Michaelis–Menten equation with an equilibrium dissociation constant for protons of pH_o = 5.3 and a Hill coefficient of 1.3. This value is significantly lower than that reported previously. To activate ASIC1, solutions must be changed very rapidly (<50 ms), otherwise the magnitude of the peak current markedly decreases. In addition, the pH_o must be returned to pH_o 7.4 after each of the test solutions for a minimum of 5 s to reactivate the channel. The latter observation indicates that the preconditioning pH_o has a profound effect on the ability to activate ASIC1. Currents were evoked by a step decrease of the preconditioning pH_o to a constant pH_o of 5.0 (Fig. 8 *Right*). Responses were normalized to the peak amplitude of current induced by decreasing the pH_o from 7.4 to 5.0. Fig. 8 *Right* shows steep inhibition in the pH_o range from 7.4 to 7.1, with complete inactivation at pH_o of 7.1. This indicates the presence of at least three states: resting, open, and inactivated. At pH_o 7.4 or higher, channels are in a resting state, which does not conduct ions. On increases in $[H^+]_o$, channels progress to the open or to the nonconducting inactivated state. Escape from inactivation is possible only by returning to pH_o above 7.4 for several seconds. The inactivated state is accessible from both resting and open states, but the transition from resting to inactivated is more sensitive to protons that the one from resting to the open.

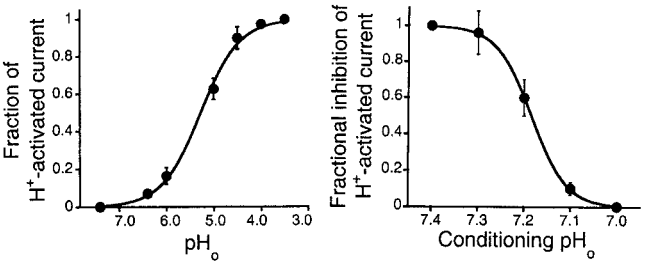

Fig. 8. Dose-response curves of activation and inactivation of ASIC1 by increasing $[H^+]_o$. Whole-cell currents from oocytes expressing ASIC1 were recorded with the two-microelectrode voltage-clamp technique. (*Left*) Currents induced by stepwise decrease in pH_o were normalized to the maximal value obtained when the pH_o was rapidly changed from 7.4 to 4.0. The solid line represents the fit of the data to the equation $I_{Max} = 1/(1 + [(K_d/pH_o)^N]$ with values for K_d of 5.3 and N of 1.3. (*Right*) Currents induced by changing the bath solution from progressively more acidic conditioning pH_o values to a constant pH_o of 5.0. Data points represent the mean ± SD of at least four oocytes.

Discussion

We have examined the distribution of the ASIC proteins in DRG neurons by using immunohistochemistry together with functional localization of unitary currents. The combined approaches strengthen the validity of our results by demonstrating the presence of the ASICs in the plasma membrane of specific cell populations. The distribution of the ASIC proteins derived from this work has important implications for the functions so far attributed to these channels.

Functional Properties and Distribution of ASIC1 in DRG Neurons. Immunohistochemistry with specific antibodies for ASIC1 and functional analysis of unitary currents indicate that ASIC1 is present in most types of sensory neurons (small, medium, and large) and coexpresses with peripherin and neurofilament 200. At the functional level, ASIC1 is found in all types of cells independent of their size. Many cells that exhibit typical ASIC1 activity also express VR1 and other types of ASIC channel, suggesting that ASIC1 preferentially forms homomeric channels in DRG.

The broad cellular distribution of ASIC1 in DRG is difficult to reconcile with its putative role in nociception (3, 24), because only a fraction of the cells that display immunoreactivity with anti-ASIC1 are involved in the perception of pain. More significant are the functional properties of ASIC1, which are characterized by much higher proton sensitivity for inactivation than for activation. Therefore, increases in $[H^+]_o$ in response to injury, ischemia, or inflammation (25, 26) will bring channels to the inactivated state, as is the case for many other cation channels in the nervous system (27, 28).

The low sensitivity of ASIC1 for protons has motivated a search for compounds that could shift the response toward a more physiological pH_o. Askwith *et al.* reported that high doses

of the peptides FF and FMRFamide prevent ASIC1 from complete inactivation and thus produce a small but sustained current (29). However, peptide-induced sustained currents occur only at very low pH_o ($pK_a \approx 5.0$), making the modulation of little physiological relevance. Even more, to elicit the sustained current, peptides had to be applied before protons. This sequence of events is also unlikely to occur under physiological conditions where ischemia and/or inflammation recruit peptides and protons simultaneously.

Functional Implications of Heteromeric ASIC2–3 Channels in Sensory Neurons. This is, to our knowledge, the first demonstration of heteromeric ASIC2–3 channels *in vivo*. By using specific antibodies, we show ASIC2 and ASIC3 predominantly in medium- to large-diameter cells from DRG, many of which also express neurofilament 200. This finding was confirmed by demonstrating functional heteromeric ASIC2–3 channels in the plasma membrane of these cells. Channels with characteristics distinctive of homomeric ASIC2 or ASIC3 were not detected either because they are expressed at low levels or because they favor association into heteromultimeric channels. Previous experiments had suggested that these proteins might associate. When the two are coinjected in oocytes, the currents are of larger magnitude and exhibit properties different from the ones in oocytes expressing ASIC2 or ASIC3 alone (16, 30). Both proteins can also be coimmunoprecipitated from cells transfected with the two cDNAs (30).

It has been proposed that ASIC2 constitutes the mammalian orthologue of the degenerins from *C. elegans*, and that it may be a mechanoreceptor. However, so far, mechanical stimuli such as cell stretch, compression, osmotic swelling, fluid shear stress, suction, or pressure applied to the membrane patch have not elicited gating in these channels. Perhaps the molecular elements that confer the responsiveness to mechanical stimuli are present in other molecules that associate with ASIC2. Nevertheless, the distribution of ASIC2 in large neurons from DRG favors a role in perception of mechanical sensory modalities. Additional support comes from functional studies on knockout mice with inactivation of the ASIC2 gene (14).

From our results, we can speculate that heteromeric ASIC2–3 are the ones involved in mechanotransduction. First, most of ASIC2, at least in the soma, seems to be associated with ASIC3. Second, cells that do not participate in propioception or tactile sensory modalities, such as motor neurons in the ventral horns of the spinal cord and Purkinje cells from the cerebellum, express ASIC2 but not ASIC3 (D.A.R. and C.M.C., unpublished observations). Finally, the finding that, in the peripheral nervous system, most ASIC2 proteins are associated with ASIC3 may also explain the absence of a distinct phenotype in the ASIC2 knockout mouse. If ASIC2–3 channels mediate mechanoperception, an intact ASIC3 gene could provide some residual function and thus account for the absence of a phenotype in these animals.

Subcellular Localization of the ASIC Proteins. The low pH for activation of the ASICs has suggested that they may reside in a low-pH intracellular compartment such as endocytic vesicles. Two publications have addressed the subcellular localization of ASIC proteins in DRG. Olson *et al.* found ASIC1 immunoreactivity in small cells that were also positive for calcitonin gene-related peptide (31). The staining appeared punctuated and within the cytoplasm but was also found in peripheral and central projections. However, the absence of proper characterization of the antibodies used in the study cast uncertainty on the validity of the conclusions. García-Añoveros *et al.* identified ASIC2a in the cytoplasm adjacent to the axon hillock; thus, they proposed that ASIC2a is transported to the peripheral terminals through the cytoplasm of the axon (19). In contrast, our results show that ASIC1, -2, and -3 are plasma membrane proteins distributed around the soma and along the axons. In addition, the high frequency of finding patches with functional ASIC channels, most of which contained multiple channels, indicates that they reside preferentially in the plasmalemma and not in intracellular compartments.

This work was supported by National Institutes of Health Grant DK17433–26 (to C.M.C.) and by the Christopher Reeves Paralysis Foundation (to F.W.).

1. Fyfe, G. K., Quin, A. M. & Canessa, C. M. (1998) *Semin. Nephrol.* **18,** 138–151.
2. García-Añoveros, J., Derfler, B., Neville-Golden, J., Hyman, B. T. & Corey, D. P. (1997) *Proc. Natl. Acad. Sci. USA* **94,** 1459–1464.
3. Waldmann, R., Champigny, G., Bassilana, F., Heurteaux, C. & Lazdunski, M. (1997) *Nature (London)* **386,** 173–177.
4. Chen, C., England, S., Akopian, A. N. & Wood, J. N. (1998) *Proc. Natl. Acad. Sci. USA* **95,** 10240–10245.
5. Price, M. P., Snyder, P. M. & Welsh, M. J. (1996) *J. Biol. Chem.* **271,** 7879–7882.
6. Lingueglia, E., de, W. J. R., Bassilana, F., Heurteaux, C., Sakai, H., Waldmann, R. & Lazdunski, M. (1997) *J. Biol. Chem.* **272,** 29778–29783.
7. Waldmann, R., Bassilana, F., de, W. J., Champigny, G., Heurteaux, C. & Lazdunski, M. (1997) *J. Biol. Chem.* **272,** 20975–20978.
8. Ishibashi, K. & Marumo, F. (1998) *Biochem. Biophys. Res. Commun.* **245,** 589–593.
9. Babinski, K., Le, K. T. & Seguela, P. (1999) *J. Neurochem.* **72,** 51–57.
10. Akopian, A. N., Chen, C. C., Ding, Y., Cesare, P. & Wood, J. N. (2000) *NeuroReport* **11,** 2217–2222.
11. Gründer, S., Geissler, H. S., Bassler, E. L. & Ruppersberg, J. P. (2000) *NeuroReport* **11,** 1607–1611.
12. Waldmann, R. & Lazdunski, M. (1998) *Curr. Opin. Neurobiol.* **8,** 418–424.
13. García-Añoveros, J. & Corey, D. P. (1997) *Annu. Rev. Neurosci.* **20,** 567–594.
14. Price, M. P., Lewin, G. R., McIlwrath, S. L., Cheng, C., Xle, J., Heppenstall, P. A., Stucky, C. L., Mannfeldt, A. G., Brennan, T. J., Drummond, H. A., *et al.* (2000) *Nature (London)* **407,** 1007–1011.
15. Rizzo, M., Kocsis, A. J. D. & Waxman, S. G. (1995) *Neurobiol. Dis.* **2,** 87–96.
16. Zhang, P. & Canessa, C. M. (2001) *J. Gen. Physiol.* **117,** 563–572.
17. Goldstein, M., House, S. B. & Gainer, H. (1991) *J. Neurosci. Res.* **30,** 92–104.
18. Guidato, S., Bajaj, P. S. N. & Miller, C. J. (1996) *Neurosci. Lett.* **217,** 157–160.
19. García-Añoveros, J., Samad, T. A., Woolf, C. J. & Corey, D. P. (2001) *J. Neurosci.* **21,** 2678–2686.
20. Akaike, N., Krishtal, O. A. & Maruyama, T. (1990) *J. Neurophysiol.* **63,** 805–813.
21. Petruska, J. C., Napaporn, J., Johnson, R. D., Gu, J. G. & Cooper, B. Y. (2000) *J. Neurophysiol.* **84,** 2365–2379.
22. Caterina, M. J., Schumacher, M. A., Tominaga, M., Rosen, T. A., Levine, J. D. & Julius, D. (1997) *Nature (London)* **389,** 816–824.
23. McIntyre, P., McLatchie, L. M., Chambers, A., Phillips, E., Clarke, M., Savidge, J., Toms, C., Peacock, M., Shah, K., Winter, J., *et al.* (2001) *Br. J. Pharmacol.* **132,** 1084–1094.
24. Sutherland, P., Benson, C. J., Adelman, J. P. & McClenskey, E. W. (2001) *Proc. Natl. Acad. Sci. USA* **98,** 711–716.
25. Krishtal, O. A. & Pidoplichko, V. I. (1981) *Neuroscience* **6,** 2599–2601.
26. Chesler, M. (1990) *Prog. Neurobiol.* **34,** 401–427.
27. Woodhull, A. M. (1973) *J. Gen. Physiol.* **61,** 607–617.
28. Tombaugh, G. C. & Somjen, G. G. (1997) *J. Physiol. (London)* **493,** 719–732.
29. Askwith, C. C., Cheng, C., Ikuma, M., Benson, C., Price, M. P. & Welsh, M. J. (2000) *Neuron* **26,** 133–141.
30. Babinski, K., Catarsi, S., Biagini, G. & Seguela, P. (2000) *J. Biol. Chem.* **275,** 28519–28525.
31. Olson, T. H., Riedl, M. S., Vulchanova, L., Ortiz-Gonzalez, X. R. & Elde, R. (1998) *NeuroReport* **9,** 1109–1113.